12

Active Materials for Photocatalytic Reduction of Carbon Dioxide

Balasubramanian Viswanathan

National Centre for Catalysis Research, Indian Institute of Technology-Madras, Chennai, India

12.1 Introduction

Solar reforming of hydrocarbons from the photocatalytic reduction of carbon dioxide is receiving considerable attention worldwide due to both the simplicity of the process and the easy manageability of the system. Carbon dioxide, a so-called greenhouse gas, was considered as a waste material until recently, but nowadays it is regarded as a good C_1 source material and thus has become to be considered to be valuable [1]. The methods of reducing carbon dioxide can be electrochemical, photochemical, photocatalytic, photoelectrochemical, and biochemical. Studies on methods for recycling carbon dioxide into useful products, such as CO, methanol, methane, formic acid, formate, and ethane, particularly using semiconductors in aqueous suspension systems, have received considerable attention in recent times. There have been many attempts to employ various means of activation to reduce carbon dioxide. These are briefly summarized in Table 12.1.

Among the various activation procedures, only a few have been vigorously pursued in view of the possibility of commercializing the developed process. Among these very few possibilities, photocatalytic or photoelectrochemical processes assume prominence.

It is known that every year, billions of metric tonnes of carbon dioxide (CO_2) are released into the atmosphere. But what if one could recycle all that CO_2 and turn it into something useful, making value-added chemicals? This desire mimics how nature converts carbon dioxide into carbohydrate by photosynthesis. Scientific pursuits often try to mimic nature, and carbon dioxide reduction is another such attempt.

Photocatalytic Functional Materials for Environmental Remediation, First Edition.
Edited by Alagarsamy Pandikumar and Kandasamy Jothivenkatachalam.

Table 12.1 The processes employed to reduce carbon dioxide to useful chemicals [53].

Process		Equation
1.	Radiochemical	$CO_2 \xrightarrow{\text{gamma-irradiation}} HCOOH,\ HCHO$
2.	Chemical reduction	$2Mg + CO_2 \rightarrow 2MgO + 2C$ $Sn + 2CO_2 \rightarrow SnO_2 + 2CO$ $2Na + 2CO_2 \rightarrow Na_2C_2O_4$
3.	Thermochemical	$CO_2 \xrightarrow{Ce^{4+};\ T>900^\circ C} CO + 1/2O_2$
4.	Photochemical	$CO_2 \xrightarrow{h\nu} CO,\ HCOOH,\ HCHO$
5.	Electrochemical	$CO_2 + xe^- + xH^+ \xrightarrow[eV]{} CO, HCOOH, (COOH)_2$
6.	Biochemical	$CO_2 + 4H_2 \xrightarrow{\text{bacteria}} CH_4 + 2H_2O$
7.	Biophotochemical	$CO_2 + \text{oxoglutaric acid} \xrightarrow{h\nu} \text{isocitric acid}$
8.	Photoelectrochemical	$CO_2 + 2e^- + 2H^+ \xrightarrow[eV,\ \text{semiconductor}]{\text{hv}} CO + H_2O$
9.	Bioelectrochemical	$CO_2 + \text{oxoglutaric acid} \xrightarrow[\text{methyl viologen}]{\text{enzyme, eV}} \text{isocitric acid}$
10.	Biophotoelectrochemical	$CO_2 \xrightarrow[eV,\ \text{methyl viologen}]{h\nu,\ \text{enzyme p-InP}} HCOOH$

By combining electricity, water, and a variety of catalysts, scientists have showed that they can reduce CO_2 into short molecules such as carbon monoxide and methane, which they can then combine to form more complex hydrocarbon fuels such as butane. Researchers think that we could now be on the cusp of a CO_2 recycling revolution, which would capture CO_2 from power plants – and maybe even directly from the atmosphere – and convert it into value-added fuels and chemicals. Strictly speaking, the photocatalytic reduction of carbon dioxide is not a catalytic process. It is an "uphill" process in that the reaction involves an energy input which may be provided by incident radiation. However, this inconsistency is often ignored and the process is still termed as "photocatalytic" and is considered as an example of artificial photosynthesis. In a broader sense, "photocatalytic" may not be very precise from a chemical point of view, but in this chapter this term is used as we look at the majority of publications in this area.

In view of the realization that photocatalytic reduction of carbon dioxide is similar to photosynthesis, even after intense research on the reduction of

carbon dioxide into value-added chemicals or fuels, the conversion levels still remain small (less than millimolar quantities) and thus not are amenable for commercial exploitation [2–4]. To utilize solar energy, the photosensitizer should absorb irradiation in the visible or ultraviolet range. Even though this process has environmental interest, the low turnover rates of the available current procedures have prevented wide-scale industrial adaptation. Lehn and Ziessel [5], in the 1980s, were the first to initiate the study of catalytic carbon dioxide reduction using visible light. They observed that Co(I) species produced in solutions containing $CoCl_2$, 2,2′-bipyridine (bpy), a tertiary amine, and a $Ru(bpy)_3Cl_2$ photosensitizer was responsible for the reduction of carbon dioxide. Subsequent to these studies, several catalysts have been reported with rhodium bipyridyl photosensitizer.

One of the issues for the low yield in the reduction of carbon dioxide is associated with the high value of the reduction potential for the initial electron transfer from the catalyst surface. That is, for the following reduction reaction

$$CO_2(aq) + e^- \rightarrow CO_2(aq)^-$$

the reduction potential value is −2.14 V versus the saturated calomel electrode (SCE) [2], even though the subsequent electron transfers may be favorable, i.e. have a more negative or positive value reduction potential with respect to the conduction band minimum of most of the semiconductor materials, a situation favorable for the feasibility of the reaction. Rapid reduction thus requires an over-potential of up to 0.6 V due to the kinetic restrictions imposed in converting the linear neutral molecule to the bent anion moiety.

The question to be answered at this stage is how this thermodynamic limitation is overcome in the product formation in photocatalytic reduction of carbon dioxide? An answer may be that photon-assisted multi-electron transfer is possible under photocatalytic reduction of carbon dioxide in aqueous solutions. However, as this complex process has to involve various reactions and each of the steps involved depends on the preference of the product to be obtained, the reduction of carbon dioxide is governed by the reduction potential values for all of these steps. A listing of reduction potential values for the photocatalytic reduction of carbon dioxide to various products in aqueous media is given in Table 12.2 [6]. This listing shows how to tune the ultimate product obtained in the photocatalytic reduction of carbon dioxide.

12.2 CO_2 Photoreduction – Essentials

The carbon dioxide photoreduction reaction in aqueous media was first reported by Inoue et al. in 1979 [7], where CO_2 was photo-reduced into organic materials, such as formaldehyde (HCHO), formic acid (HCOOH), methanol (CH_3OH),

Table 12.2 Reduction potential values for carbon dioxide. The value for hydrogen production from water is included for comparative purposes and its relevance in CO_2 reduction.

Reaction	E°_{redox} (eV)
$CO_2 + e^- \rightarrow CO_2^-$	≥−1.9
$CO_2 + 2H^+ + 2e^- \rightarrow HCOOH$	−0.61
$CO_2 + 2H_2O + 2e^- \rightarrow HCOOH^- + OH^-$	−1.491
$CO_2 + 2H^+ + 2e^- \rightarrow CO + H_2O$	−0.53
$CO_2 + 2H_2O + 2e^- \rightarrow CO + 2OH^-$	−1.347
$2CO_2 + 2H^+ + 2e^- \rightarrow H_2C_2O_4$	−0.913
$2CO_2 + 2e^- \rightarrow C_2O_4^{2-}$	−1.003
$CO_2 + 4H^+ + 4e^- \rightarrow C + 2H_2O$	−0.20
$CO_2 + 4H^+ + 4e^- \rightarrow HCHO + H_2O$	−0.48
$CO_2 + 3H_2O + 4e^- \rightarrow HCHO + 4OH^-$	−1.311
$CO_2 + 2H_2O + 4e^- \rightarrow C + 4OH^-$	−1.040
$CO_2 + 6H^+ + 6e^- \rightarrow CH_3OH + H_2O$	−0.38
$CO_2 + 5H_2O + 4e^- \rightarrow CH_3OH + 6H_2O$	−1.225
$CO_2 + 8H^+ + 8e^- \rightarrow CH_4 + 2H_2O$	−0.24
$CO_2 + 6H_2O + 8e^- \rightarrow CH_4 + 8OH^-$	−1.072
$2CO_2 + 12H^+ + 12e^- \rightarrow C_2H_4 + 4H_2O$	−0.349
$2CO_2 + 8H_2O + 12e^- \rightarrow C_2H_4 + 12OH^-$	−1.177
$2CO_2 + 12H^+ + 12e^- \rightarrow C_2H_5OH + 3H_2O$	−0.329
$2CO_2 + 9H_2O + 12e^- \rightarrow C_2H_5OH + 12\ OH^-$	−1.157
$2CO_2 + 14H^+ + 14e^- \rightarrow C_2H_6 + 4H_2O$	−0.270
$3CO_2 + 18H^+ + 18e^- \rightarrow C_3H_7OH + H_2O$	−0.310
$2H^+ + 2e^- \rightarrow H_2$	−0.42
$3CO_2 + 18H^+ + 18e^- \rightarrow CH_3CH(OH)CH_3 + 5H_2O$	−0.30
$2CO_2 + 10H^+ + 10e^- \rightarrow CH_3CHO + 3H_2O$	−0.36
$3CO_2 + 16H^+ + 16e^- \rightarrow CH_3CH_2CHO + 5H_2O$	−0.32
$3CO_2 + 16H^+ + 16e^- \rightarrow CH_3COCH_3 + 5H_2O$	−0.31
$2CO_2 + 8H^+ + 8e^- \rightarrow CH_3COOH + 2H_2O$	−0.31

Source: Values collected from Ref. [6].

and hydrocarbons (such as methane, CH_4, and ethane, C_2H_6) by using semiconductor photocatalysts. When the semiconductor is exposed to irradiation, it absorbs appropriate photon energy ($h\nu$) corresponding to the bandgap or higher.

Then, if the absorbed photon energy is sufficient to overcome the bandgap of the semiconductor (the forbidden or void energy region that extends from the top of the filled valance band to the bottom of the vacant conduction band) the electrons (e–) in the valence band (VB) can be excited and transferred to the conduction band (CB), leaving positively charged holes (h^+) in the VB. These photo-generated electron and hole pairs (e^-/h^+) may move to the surface of the semiconductor and react with the adsorbed species (e.g. CO_2, H_2O) to initiate the CO_2 photoreduction.

It should be realized that the photogeneration of electron and hole pairs is a reversible process, and these electron and hole pairs may undergo bulk or surface recombination, emitting photon and heat energy. Such a recombination process can inhibit electron and hole pairs participating in surface reactions for CO_2 photoreduction. Therefore, a decrease of the electron and hole recombination rate can increase the lifetime of these charge carriers and significantly improve the efficiency of CO_2 photoreduction. A pictorial representation of the photocatalytic process is shown in Figure 12.1.

It can be seen that CO_2 photoreduction with water requires both multi-electron transfer reactions and water oxidation and they have to occur simultaneously. The band-edge energy positions of the VB and CB of the

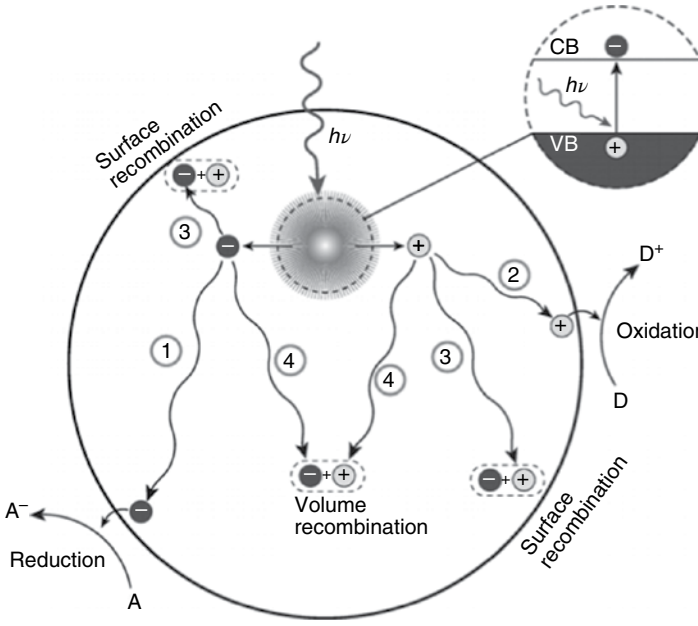

Figure 12.1 Schematic diagram of photoexcitation and electron-transfer processes in a semiconductor. *Source:* Adapted and reproduced from Refs. [21, 74]. The numbers 1, 2, 3, and 4 inside circles denote the migration of charge carriers inside the semiconductor.

semiconductor are critical to determine whether these reactions can be initiated. The band-edge position of the VB must be sufficiently positive to allow the photo-generated hole to initiate the necessary oxidation (e.g. more positive than the redox potential of H_2O decomposition). Meanwhile, the band-edge position of the CB must be sufficiently negative to allow the photo-generated electron to participate in the reduction reactions (e.g. more negative than the redox potential of CO_2, for example reduction into CH_4, –0.24 V). Moreover, based on the redox potentials, CO_2 photoreduction may be more favorable to be a multi-electronic process which yields the final products, such as methane, methanol, formaldehyde, formic acid, carbon monoide or others, through different intermediates. The various reduction processes that can take place through the photocatalytic reduction of carbon dioxide are already listed in Table 12.2. Depending on the nature of the semiconductor, a specific reduction product can be selectively formed on a given semiconductor.

Although low yields in the photocatalytic reduction of carbon dioxide are observed, encouraging laboratory experimental results have been obtained in both gas and liquid phases. Semiconductor-based systems, metal–organic frameworks (MOFs), and composites involving C_3N_4 and MoS_2 have been examined for the photocatalytic reduction of carbon dioxide. Semiconductor heterostructures, containing bimetallic alloys and chemical modification of oxides with anion substitution (N^{3-} and F^- in place of O^{2-}), have also been tried as possible catalytic candidates.

12.3 Heterogeneous Photocatalytic Reduction of Carbon Dioxide with Water

In the photocatalytic reduction of carbon dioxide with water, both the photoreduction of carbon dioxide and the photooxidation of water take place simultaneously under sunlight irradiation, employing a photocatalyst. Since a variety of reaction conditions affect the reaction, predicting the product distribution on a catalyst system is often a difficult proposition, though it is feasible [6].

Photocatalytic reduction of carbon dioxide is one of the pathways involved in the carbon dioxide conversion process and has been receiving considerable attention from the scientific community in the last few decades. The mechanism of carbon dioxide reduction is not still clear and the information available is not sufficient for developing it into large-scale commercially viable applications, possibly because of the innumerable hurdles associated with the reduction process. The reductive photocatalytic conversion of CO_2 involves all the redox reactions occurring at the interface of the semiconductor, such as water splitting, hydrogen evolution, oxygen evolution, photooxidation reactions, and reactions of radical intermediates. The overall product yield is highly dependent on the extent of these competing reactions [8].

The work by Lehn et al. showed the selective CO_2 reduction into CO by using Re(I) diimine complexes [5, 9]. Subsequently, metal complexes in photocatalysis have been studied for both CO_2 reduction [10–13] and H_2O oxidation [14–16]. CO_2 is reduced to form CO with homogeneous photocatalysts, such as Re complexes; however, efficiency of the process increased in the presence of electron donors, such as triethanolamine [17, 18]. However, CO_2 reduction and H_2O oxidation processes require distinct and possibly separate reaction conditions. As a result, carrying out these reactions simultaneously using a metal complex catalyst in a single system is a difficult task. Reverse oxidation of organic products generated from the reduction of CO_2 and the reverse reduction of O_2 generated from the oxidation of H_2O may terminate the continuity of the reaction. Catalysis by metal complexes will not be further considered here, as the scope of this chapter is only to examine the heterogeneous photocatalytic reduction of carbon dioxide by semiconducting materials. It could be questioned as to why one should restrict consideration only to semiconducting materials, especially for a globally important reaction such as carbon dioxide reduction. A limited answer to this point is that the literature is vast if one were to consider all the information, and also there appears to be vast choice of materials among the literature. Any successful direction in the literature will go a long way in attempting to commercialize this process.

The reduction potentials for the proton-coupled electron transfer (PCET) reactions of carbon dioxide are within the range of −0.7 to −0.2 V (see Table 12.2) and are close to the reduction potential of water (−0.414 V at pH 7). Gas phase carbon dioxide is a linear molecule; when it is adsorbed on the catalyst surface the bond angle is reduced from 180° and thus becomes susceptible for reduction. The values of the reduction potentials of carbon dioxide are given in Table 12.2 and generally refer to multi-electron/proton transfer reactions as compared to water decomposition. Water decomposition is a two-electron transfer reaction and hence in the liquid phase hydrogen generation from water can be facile compared to the reduction of carbon dioxide. This may account for the low yields obtained in the experiments on the reduction of carbon dioxide in the presence of water decomposition. However, the solubility of carbon dioxide in water is small, being of the order of $\sim 5.4–6 \times 10^{-4}$ mol fraction of carbon dioxide [19] in liquid phase at around atmospheric pressure. The solubility of CO_2 in water can be improved by the addition of substances such as NaOH, $NaHCO_3$, or Na_2CO_3.

It is normal to use sacrificial reagents to consume the generated holes. The addition of a sacrificial reagent to the reaction mixture enhances photocatalytic reduction. For example, methanol is used as a sacrificial hole scavenger. This implies that some of the CO_2 reduction products are formed through the action of holes and not the action of electrons. The presence of organic adsorbents (CH_3CO_2H, CH_3OH, HCO_2H) on the surface of the photocatalyst plays an important role in the photoreduction of CO_2. The presence of acetic acid on

the photocatalyst surface leads to the formation of CH_4. This can occur by the conversion of acetic acid to CH_4 via the photo-Kolbe reaction.

It has been already stated that the deviation of the bond angle from 180° is essential in activating carbon dioxide and facilitates its reduction. This implies that the adsorption sites should be such that the bond angle of linear carbon dioxide is reduced from the value of 180°. One such visualization has been made in the literature and is shown in Figure 12.2. This type of site may be present on stepped surfaces of semiconductors. Other geometrical arrangements are possible for the adsorption and activation of carbon dioxide [20].

Fujishima, Honda, and their co-workers reported the photocatalytic reduction of CO_2 to organic compounds, such as HCOOH, CH_4, CH_3OH, and HCHO, in the presence of semiconductor photocatalysts such as TiO_2, ZnO, CdS, SiC, and WO_3 [7]. Heterogeneous semiconductor compounds, including metal oxides, oxynitrides, sulfides, and phosphides, had been investigated for this purpose [21, 22].

The photocatalytic CO_2 reduction is a useful method since no additional energy is needed and there is little negative effect on the environment. The use of cheap and abundant sunlight to convert a greenhouse gas into other carbon-containing products is also an ideal approach. Some of the typical semiconductors employed for the study of this reaction are assembled in Table 12.3.

12.4 Nanomaterials and New Combinations of Materials for Carbon Dioxide Reduction

In this section, a brief description of nanomaterials is given and we look at how useful they are for the photocatalytic reduction of carbon dioxide. One-dimensional (1D) nanomaterials with different morphologies and high surface areas have been shown to facilitate electron transport and also to minimize the loss of charge carriers [23]. Among the 1D nanostructures, highly ordered

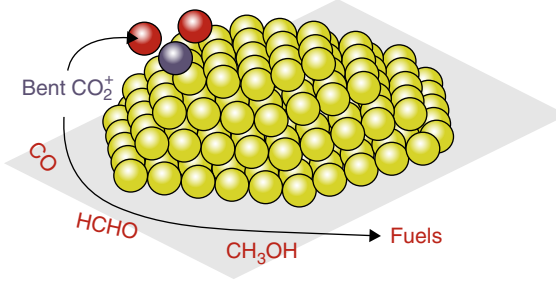

Figure 12.2 One adsorption geometry for carbon dioxide that facilitates its reduction.
Source: Reproduced from Ref. [75].

Table 12.3 Typical semiconductors used for the photoreduction of carbon dioxide.

Semiconductor	Bandgap (eV)	Description	Ref.
TiO_2	3.2	UV, λ = 365 nm, λ = 254 nm, methane, CO, and other products	[54–58]
Graphene-TiO_2		methanol and formic acid, under light of 365 nm, can reach 160 and 150 μmol g^{-1}	[59]
ZnO	3.44	CO formation rate (3.814 μmol $g^{-1}h^{-1}$) in comparison with ZnO microspheres and ZnO microflowers (3.357 and 1.627 M mol g^{-1} h^{-1}, respectively)	[60, 61]
CdS	2.42	methanol nearly 40 μmol g^{-1} h^{-1}; CdS on MMT, the product yield $H_2 > CH_4 > CO$	[61, 62]
Bi_2O_3	2.8	methanol nearly 60 μmol $g^{-1}h^{-1}$	[62]
SiC	3.0	HCOOH, HCHO, and CH_3OH are the main products	[7]
u–g–C_3N_4 (Cu loaded)	2.75	better performance in photocatalytic carbon dioxide reduction, methane is major product	[61, 63]
ZrO_2	5.0	rates of gas evolutions were 19.5 μmol h^{-1} of H_2, 10.8 μmol h^{-1} of O_2, and 2.5 μmol h^{-1} of CO	[64, 65]
Ta_2O_5-rG		high methanol yields	[61]
ZnS	3.91	CO_2 reduced to HCOOH, ZnS–MMT (montmorillonite) nanocomposite exhibited 5–6-fold higher efficiency of photocatalytic CO_2 reduction	[8, 61, 66]
GaN	3.4	the reduction of CO_2 to CO dominates on as-grown GaN nanowires under ultraviolet light irradiation	[65]
GaP	2.16	HCOOH, HCHO, and CH_3OH are the reported products	[8]
GaAs	1.43	spontaneously produce CH_3OH, even under conditions of no net current	[67]
PbS	0.37	The PbS QDs enhance CO_2 photoreduction rates with TiO_2 by a factor of ~5 in comparison to unsensitized photocatalysts	[68]
$SrTiO_3$	3.3	7 μmol h^{-1} methanol and less than 1 μmol h^{-1} formaldehye	[69]
$LiNbO_3$	4.0	lithium niobate achieved unexpectedly high conversion of CO_2 to products despite the low levels of bandgap light available.	[70]

(Continued)

Table 12.3 (Continued)

Semiconductor	Bandgap (eV)	Description	Ref.
MoS_2	1.23	compared with the pristine Bi_2S_3 or MoS_2, the as-synthesized D-Bi_2S_3@MoS_2 composite has exhibited much higher adsorption behavior and photocatalytic activity under visible light irradiation	[71]
$BaLa_4Ti_4O_{15q}$	~4 and 5	H_2: 10 μmol h^{-1}, O_2: 7 μmol h^{-1}, CO: 4.3 μmol h^{-1}, HCOOH: 0.3 μmol h^{-1}	[68]
$KTaO_3$	~3.5	reduce CO_2 to CO and oxidize water to O_2	[72]
WO_3 and graphene-WO_3	2.8	around 5 μmol h^{-1} methanol	[61, 69]

vertical TiO_2 nanotube arrays (NTAs) have shown significant photocatalytic activity of CO_2 reduction [24, 25]. However, maintaining the long-time stability and high activity of the catalyst, especially the co-catalyst, is still a great challenge. Noble metal Pt nanoparticles (NPs) are easily poisoned by CO during the catalytic process [26] and for non-noble metal NPs, changes in the surface states [27] are the main reason for the co-catalyst deactivation.

Efficient photocatalytic conversion of CO_2 into CO and hydrocarbons by hydrous hydrazine ($N_2H_4{\cdot}2H_2O$) is shown on $SrTiO_3/TiO_2$ coaxial NTAs loaded with Au/Cu bimetallic alloy. The synergetic catalytic effect of the Au/Cu alloy nanoparticles and the facile electron transfer in the $SrTiO_3/TiO_2$ coaxial nanoarchitecture are the reasons for the efficiency. The reduction products are identified by IR spectroscopy [28]. By varying the fraction of one component in this bimetallic alloy system, a $Au_3Cu@STO_3/TiO_2$ NTA has been found that is the most reactive photocatalyst in this family to generate hydrocarbons from diluted CO_2 with $N_2H_4{\cdot}2H_2O$ acting as the hydrogen source and electron donor and also providing a reductive atmosphere for maintaining the alloying system.

Plasmonic photocatalysts have become popular in recent times [29–31]. This is because nano metals such as Au, Ag, and Pt exhibit strong absorption in the UV-vis region due to their surface plasmon resonance (SPR) [32]. SPR means the collective oscillations of conduction band electrons in a metal particle and it is driven by the electromagnetic field of incident light [33, 34]. Dispersing metal nanoparticles (10–100 nm) on a semiconductor photocatalyst shows significant enhancement in photocatalytic activity under UV and visible light irradiation due to SPR.

The surface plasmonic resonance frequency can be tuned by manipulating the size, shape, and material of the nanoparticles. Noble metal nanoparticles are a combination of surface area and active sites. In the photocatalytic CO_2

reduction with water, it has been reported that depositing Au nanoparticles on TiO_2 results in plasmonic enhancement (532 nm) of a 24-fold enhanced photocatalytic activity. The synthesis, characteristics, and application of plasmonic photocatalysts in CO_2 reduction with H_2O, where CH_4 and CO are produced under visible light irradiation (>400 nm wavelength) has also been reported. The comparative photocatalytic activities toward the CO_2 reduction of a different photocatalyst in the presence of water under visible light were evaluated by the quantity of carbon-containing products. The results show the increasing amount of CH_4 and CO formation with time under visible light.

There are various ways, as shown above, that carbon dioxide can be reduced to value-added chemicals and fuels. In all these attempts, it is the selection of materials to promote the reaction in the desired direction that appears to be both critical and challenging [35]. Many developments have been carried out in the photocatalytic reduction of carbon dioxide. Recently, it has been shown that even infrared radiation can be effectively utilized, using an oxygen-deficient WO_3 system to reduce CO_2 [36]. The pictorial representation of this process that has been proposed [36] is reproduced in Figure 12.3. These developments show that though the conversion levels of carbon dioxide is low at present, it is certain that, in the near future, the conversion of carbon dioxide into value-added chemicals and fuels will become a commercially viable process. However, this exploitation requires that some fundamental principles are fully understood and the material selection is made on a rational basis.

Only a few of the variations in the choice of materials or combinations will be considered in this section. In a recent publication [37], the photosynthetic

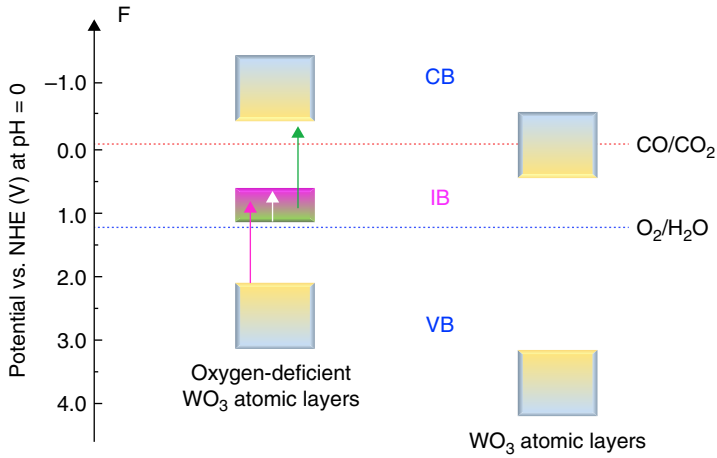

Figure 12.3 Energy level diagram of layers and oxygen-deficient WO_3 atomic layers which can be used with the infrared radiation of solar radiation for the photocatalytic reduction of carbon dioxide. *Source:* Reproduced from Ref. [36].

conversion of carbon dioxide to hydrocarbons (methane and other higher hydrocarbons) on Pd/TiO_2 in conjunction with Nafion has been reported. The conversion efficiency of this process is, as usual, not high. Since the one-electron reduction of CO_2 (the initial step in the reduction process) requires high potentials of the order of 2 V (as pointed out earlier in this chapter), a favorable pathway is to reduce CO_2 though PCETs. The role of the Nafion layer is to enhance the local proton activity within the layer to facilitate PCET reactions, to stabilize intermediates, and to inhibit the re-oxidation of the CO_2 reduction products. It is observed that Nf/Pd–TiO_2 is more active than Pd–TiO_2 for the photoproduction of hydrocarbons (e.g. methane, ethane, and propane). The conceptual design of the catalyst system employed in this study is shown in Figure 12.4 [37].

In the light of these results, the following points are presented for conceptual analysis and possible adaptation.

i) Is a direct proton source desirable (rather than the protons coming from the decomposition of water), so that the reduction of CO_2 is facilitated?
ii) It is essential that the species employed as a proton source should not undergo any electrochemical reaction within the potential range for the CO_2 reduction reaction.
iii) The reactivity of the proton should be as high as that in Nafion (very nearly a bare proton), where the proton is in a highly electronegative environment of fluorine atoms.
iv) The available protons should be capable of reacting with carbon dioxide directly, promoted by the light absorbed by semiconductors (TiO_2), and the reduction reaction should be carried out on some reactive metal sites. This possibly means the photon absorption and reactive sites may be distinguishable.

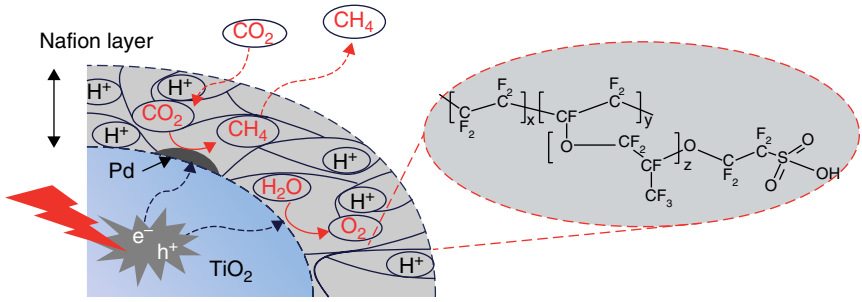

Figure 12.4 Pd/TiO_2 on Nafion catalyst system for the photochemical reduction of carbon dioxide. *Source:* Reproduced from Ref. [37] with permission from the Royal Society of Chemistry.

Considering these aspects, and also based on argumentative considerations, it is possible that alternative PCET catalyst support systems that may sustain more acidic protons can be tried, such as heteropoly acids or super acids (such as sulfated zirconia).

Another opinion in material selection in recent times is the hybrid perovskites ($CH_3NH_3PbI_3$) as a possible alternative for solar cell and photocatalytic applications. These materials have been shown to be nearly two times more active (24%) as compared to kesterite ($Cu_2ZnSn(S,Se)_4$) materials [38], while the number of publications about hybrid perovskites is nearly three times the number of those on kesterite. It may be presumed that kesterite may become one of the possible alternative materials for the photocatalytic reduction of carbon dioxide in the near future. In the next decade, there is the possibility that the efficiency of these materials may improve and thus pave the way for the commercialization of this process.

Many more variations are being tried to increase the useful photon energy range into the visible and near infrared, as well as to increase the efficiency of the process. These attempts are continuing exercises in research, and will continue to be, until a viable and efficient system has been identified.

12.5 Selection of Materials

It is realized that in any successful attempt to make this process viable commercially, the selection of photocatalytic material is an important requirement. There have been various attempts in this direction in the past based on various methodologies. However, even today, the search continues to identify a material which will be able to provide the efficiency required. In this connection it has been pointed out earlier that the positions of the conduction band minimum and valence band maximum of the semiconductor represent the reduction and oxidation ability of the system. A compilation of the known semiconductors and their characteristics is attempted in Table 12.4. The data presented in this table may be useful in order to select a semiconductor material based on the logistics of the process instead of on a trial and error basis. This is an important aspect, since the selection of suitable materials is the immediate need for making this process commercially viable and environmentally acceptable. Note that in the two "Band edge" columns in Table 12.4, the figures in brackets are the pH value at which the band edges values are reported if this isn't pH 7. The values given in Table 12.4 can be used to identify appropriate and suitable semiconductor materials for the simultaneous photocatalytic reduction of carbon dioxide and photodecomposition of water.

Table 12.4 List of semiconductors with data on bandgap, valence band maximum, and conduction band minimum.

Name	Formula	E_g (eV)	CB edge at pH = 7 (eV)	VB edge at pH = 7 (eV)	λ (nm)
aluminum oxide	Al_2O_3	7.1	−3.6	3.5	175
antimony oxide	Sb_2O_3	3.00	0.32	3.32	413
antimony sulfide	Sb_2S_3	1.72	0.22	1.94	
arsenic sulfide	As_2S_3	2.50	0.08	2.58	496
barium titanate	$BaTiO_3$	3.30	0.08	3.38	376
barium titanate	$BaTiO_3$	3.30	−3.4	0.1	376
bismuth niobium oxychloride	Bi_4NbO_8Cl	2.39	−2.11	0.28	519
bismuth oxide	Bi_2O_3	2.80	0.33	3.13	443
bismuth oxychloride	BiOCl	3.42	−1.5	1.92	363
bismuth vanadate	$BiVO_4$	2.4	−0.3	2.1	517
boron carbon nitride	h-BCN	2.82	−1.59	1.23	440
cadmium ferrite	$CdFe_2O_4$	2.30	0.18	2.48	539
cadmium oxide	CdO	2.20	0.11	2.31	564
cadmium selenide	CdSe	2.0	1.2	3.2	620
cadmium sulfide	CdS	2.4	−0.6	1.8	517
cadmium sulfide	CdS	2.40	−0.52	1.88	517
cerium oxide	Ce_2O_3	2.40	−0.50	1.9	517
chromium oxide	Cr_2O_3	3.50	−0.57	2.93	354
cobalt oxide	CoO	2.01	−0.11	1.9	617
cobalt titanate	$CoTiO_3$	2.25	0.14	2.39	551
copper iron sulfide	$CuFeS_2$	0.35	0.47	0.82	—
copper oxide	CuO	1.70	0.46	2.16	729
copper(II) oxide	CuO	1.35	4.07	5.42	1032
copper titanate	$CuTiO_3$	3.0	−0.18	2.81	413
copper titanate	$CuTiO_3$	2.99	−0.18	2.81	415
cuprous oxide	Cu_2O	1.9	−1.30	0.60	620
cuprous oxide	Cu_2O	2.20	−0.28	1.92	564
$FAPbI_3$	$FAPbI_3$	1.5	−5.42	−3.92	827
ferric oxide	Fe_2O_3	2.2	0.13	2.33	560
ferric oxide	Fe_2O_3	2.20	0.28	2.48	564
ferrous ferric oxide	Fe_3O_4	0.10	1.23	1.33	—

Table 12.4 (Continued)

Name	Formula	E_g (eV)	CB edge at pH = 7 (eV)	VB edge at pH = 7 (eV)	λ (nm)
ferrous sulfide	FeS	0.10	0.47	0.57	—
gallium oxide	Ga_2O_3	4.80	−1.54	3.26	258
indium oxide	In_2O_3	2.9	−3.88 (at pH 8.64)	−0.98	428
indium oxide	In_2O_3	2.80	−0.62	2.18	443
indium sulfide	In_2S_3	2.00	−0.80	1.20	620
indium tantalum oxide	$InTaO_4$	2.6	−0.75	1.85	477
iron disulfide	FeS_2	0.95	0.42	1.37	—
iron titanate	$FeTiO_3$	2.80	−0.21	2.59	443
iron(II) oxide	FeO	2.40	−0.17	2.23	517
lanthanum oxide	La_2O_3	5.50	−1.97	3.53	227
lead copper antimony sulfide	$PbCuSbS_3$	1.50	0.11	1.61	
lead oxide	PbO	2.80	−0.48	2.32	443
lead sulfide	PbS	0.37	0.24	0.61	
lead titanate	$PbTiO_3$	2.75	−2.75	0.0	451
lithium niobate	$LiNbO_3$	3.50	−0.73	2.77	354
lithium tantalate	$LiTaO_3$	4.00	−0.95	3.05	310
magnesium oxide	MgO	7.3	−3.0	4.3	159
magnesium titanate	$MgTiO_3$	3.70	−0.75	2.95	335
manganese dioxide	MnO_2	0.25	1.33	1.58	
manganese disulfide	MnS_2	0.50	0.49	0.99	—
manganese oxide	MnO	3.60	−1.01	2.59	344
manganese(II) oxide	MnO	3.6	−3.49 (at pH 8.61)	0.11	345
manganese sulfide	MnS	3.00	−1.19	1.81	413
manganese titanate	$MnTiO_3$	3.10	−0.46	2.64	400
mercury oxide	HgO	1.90	0.63	2.53	653
methyl lead bromide	$MaPbBr_3$	2.3	−5.68	−3.38	539
methyl lead chloride	$MAPbCl_3$	3.09	−2.54	0.55	400
methyl lead iodide	$MAPbI_3$	1.55	−5.43	−3.88	800
methyl tin iodide	$MASnI_3$	1.3	−5.47	−4.17	954
molybdenum sulfide	MoS_2	1.17	0.23	1.40	

(Continued)

Table 12.4 (Continued)

Name	Formula	E_g (eV)	CB edge at pH = 7 (eV)	VB edge at pH = 7 (eV)	λ (nm)
nickel disulfide	NiS_2	0.30	0.89	1.19	
nickel oxide	NiO	4.3	–0.5	3.8	285
nickel oxide	NiO	3.50	–0.50	3.0	413
nickel sulfide	NiS	0.40	0.53	0.97	
nickel titanate	$NiTiO_3$	2.18	0.20	2.38	569
nickel titanate	$NiTiO_3$	2.18	0.20	2.38	569
niobium oxide	Nb_2O_5	3.40	0.09	3.49	365
niobium pentoxide	Nb_2O_5	3.40	0.09	3.49	365
palladium oxide	PdO	1.00	0.79	1.79	1240
platinum sulfide	PtS_2	0.95	1.03	1.98	
potassium niobate	$KNbO_3$	3.30	–0.86	2.44	376
potassium tantalate	$KTaO_3$	3.50	–0.93	2.57	354
rhodium sulfide	Rh_2S_3	1.50	0.11	1.61	
ruthenium sulfide	RuS_2	1.38	0.39	1.77	
silicon	Si	1.1	–0.6	0.5	1125
silicon carbide	SiC	3.0	–1.5	1.5	415
silver oxide	Ag_2O	1.20	0.19	1.49	1033
silver sulfide	Ag_2S	0.92	0.0	0.92	1348
strontium titanate	$SrTiO_3$	3.4	–3.24 (at pH 8.6)	0.16	364
strontium titanate	$SrTiO_3$	3.40	–1.26	2.14	365
tantalum oxide	Ta_2O_3	4.00	–0.17	3.83	310
tin dioxide	SnO_2	3.50	0.0	3.5	354
tin oxide	SnO_2	3.5	–4.5 (at pH 4.3)	–1.0	354
tin oxide	SnO	4.20	–0.91	3.29	295
tin sulfide	SnS	1.01	0.16	1.17	
titanium oxide (anatase)	TiO_2	3.23	–0.29	2.94	384
titanium oxide (rutile)	TiO_2	3.02	–0.52	2.5	410
titanium sulfide	TiS_2	0.70	0.26	0.96	
tungsten oxide	WO_3	2.6	0	2.5–2.8	495–442
tungsten oxide	WO_3	2.70	0.74	3.44	459
tungsten selenide	WSe_2	1.4	–0.25	1.15	1032

Table 12.4 (Continued)

Name	Formula	E_g (eV)	CB edge at pH = 7 (eV)	VB edge at pH = 7 (eV)	λ (nm)
tungsten sulfide	WS_2	1.35	0.36	1.71	
vanadium pentoxide	V_2O_5	2.7	−4.7 (at pH 6.54)	−2.0	458
vanadium pentoxide	V_2O_5	2.80	0.20	3.0	443
zinc indium sulfide	$Zn_3In_2S_6$	2.81	−0.91	1.90	441
zinc oxide	ZnO	3.2	−0.31	2.91	387
zinc oxide	ZnO	3.20	−0.31	2.89	388
zinc sulfide	ZnS	3.7	−3.46 (at pH 1.7)	0.24	335
zinc sulfide	ZnS	3.60	−1.04	2.56	344
zinc titanate	$ZnTiO_3$	3.07	−0.23	2.84	404
zirconium dioxide	ZrO_2	5.00	−1.09	3.9	248
zirconium sulfide	ZrS_2	1.82	−0.21	1.61	681

Source: data collected from literature, especially from Refs. [4, 73], among others.

12.6 Material Modifications for Improving Efficiency

According to the given description of the mechanism of carbon dioxide photoreduction, it can be stated that the selection of the semiconductor photocatalyst is the key for the success of this process. The semiconductor photocatalyst suitable for carbon dioxide photoreduction should not only provide appropriate valence bands and conduction bands with suitable energy positions that can induce water decomposition and carbon dioxide reduction reactions simultaneously, but also have the properties of chemical stability and low cost [39]. According to the research reported so far, all these factors have been found in only one material, which is titanium dioxide (TiO_2). This is the most widely used semiconductor, and it has been claimed to be one of the best options to act as a photocatalyst for CO_2 photoreduction [40, 41]. Two common crystalline structures of TiO_2, rutile and anatase, are commonly used in photocatalysis, with anatase showing a higher photocatalytic activity. This may be because of the relatively larger bandgap of anatase (3.2 eV) than that of rutile (3.0 eV), which allows anatase to provide more sufficiently negative and positive redox potentials in CB and VB during photocatalysis. Hence, most of the reports on TiO_2 have shown that the anatase form successfully initiates CO_2 photoreduction. However, there are aspects of anatase which have to be improved before it can be exploited for use in a commercial process for the conversion of carbon dioxide.

However, there are still disadvantages hindering the use of TiO_2 as an effective catalyst for CO_2 photoreduction. Firstly, the efficiency of CO_2 photoreduction using TiO_2 is still too low for practical applications. It can be seen that even the best work could only achieve a CO_2 conversion rate at around $26\,\mu mol\,g^{-1}\,h^{-1}$ [40]. Such reaction efficiency is obviously too low for practical applications and, therefore, it is necessary to improve the activity of TiO_2 or find alternative materials for carbon dioxide photoreduction.

Yet another problem when using TiO_2 is its relatively large bandgap (3.2 eV) that can only be effectively excited by ultraviolet (UV) light. As only small fraction of the solar spectrum is within the UV region (not higher than 3%), there is a need to modify the light absorption range of TiO_2 to efficiently utilize solar energy for CO_2 photoreduction. One of the most widely used methods to improve the activity of TiO_2 for CO_2 photoreduction is by modifying TiO_2 with a metal. This is because the added metal is able to act as a trap of the photogenerated charge carriers in order to suppress the electron/hole recombination rate and improve the activity of TiO_2.

Metal loading on or in a semiconductor can either create alternate adsorption sites or alter the electronic energy levels, thus facilitating the electron-transfer reactions. (Metal can be loaded on the surface and not incorporated into the lattice, or it can be loaded in the lattice, in which case the doped metal can give rise to additional allowed energy levels in the so-called forbidden gap or can alter the Fermi level of the semiconductor by charge injection into the host lattice.) Thus, metal loading on to a semiconductor may function as electron traps, thereby suppressing electron/hole recombination rate and thus promoting the desired reaction. This process increases the possibility of these charge carriers reacting with the adsorbed species on the metallic sites that are loaded on the semiconductor photocatalyst. If the loaded metal undergoes oxidation due to calcination, then what one gets is a coupled/composite semiconductor system which also experiences Fermi-level equalization due to intimate contact. When the added metal is doped into the lattice of the semiconductor (TiO_2), the doping can be either substitutional or interstitial. Both of these two types of doping can affect the lattice spacing of TiO_2. Incorporation in the substitutional position or interstitial position is reflected in the variation of the lattice spacing of the parent semiconductor. Additional allowed energy levels in the forbidden gap of the semiconductor depends on their energy positions, can act as electron or hole traps, and promotes the corresponding reduction or oxidation reactions or facilitates the recombination of the charge carriers. Hence, the ratio of the doped metal to that of the parent semiconductor must be carefully considered, because the presence of the metal dopant can simultaneously suppress and enhance the recombination of the photo-generated electron and hole within the semiconductor. It has been reported in the literature that incorporation of metals such as Cu, Pt, Pd, Rh, Fe, and Ag into TiO_2 can improve the photocatalytic reduction of carbon dioxide. All these studies can be generally understood by

the "metal-modified TiO_2" terminology instead of specifying them as either doping or metal loading.

TiO_2 has been chosen as a representative system. The modifications that have been described, namely doping and coupling, are general in nature and applicable to all the semiconductors that have been tried for this photocatalytic reaction. These studies been attempted in many other semiconductor systems, as shown in Table 12.4. In spite of the many variations that have been tried, the efficiency of the resultant systems has not improved to the desired level and thus the exercise to identify the selection of materials with optimum efficiency is still continuing. These studies that covered the TiO_2 system are equally applicable to other systems as well and hence they are not covered in this chapter.

To summarize the reactions on semiconductor surfaces, the reduction potentials for various reaction products in the photocatalytic reduction of carbon dioxide are shown in Figure 12.5. On the left-hand side the potential scale is with zero at vacuum and on the right-hand side the electrochemical scale is shown at pH = 0.

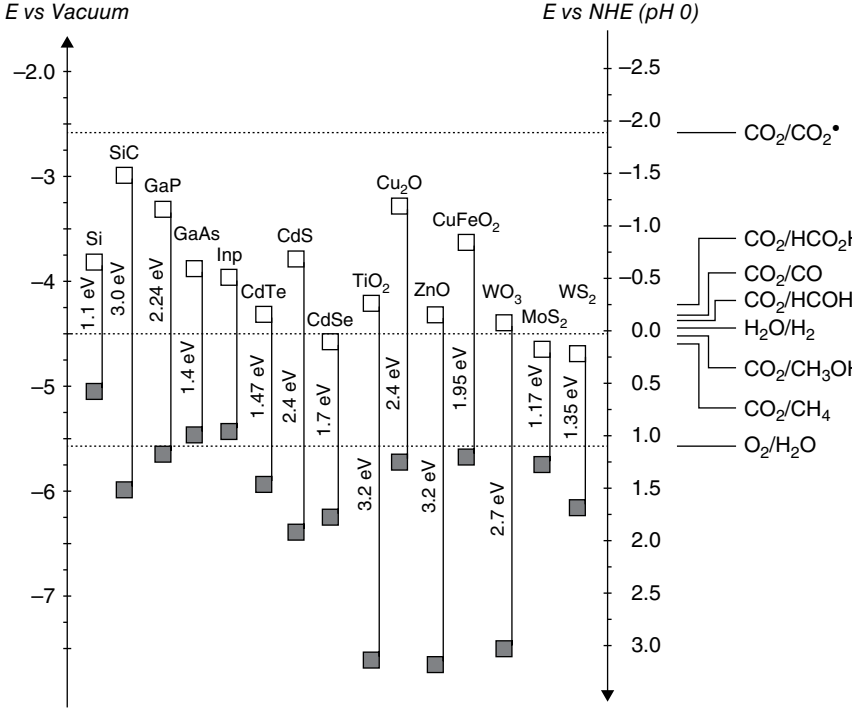

Figure 12.5 Conduction band potentials (open squares) and valence band potentials (gray squares) of some commonly used semiconductors, along with with the potentials of several carbon dioxide/water redox couples at pH = 0.

The efforts extended in making this process more efficient have not so far yielded the desired results. This probably indicates that the basic choice of materials has not been appropriate. In spite of the concerted efforts to modify and redesign the available known materials, perhaps one now has to focus on completely new materials for this reaction. It has been pointed out already that the energetic position of the conduction band and the valence band controls the reduction and oxidation reactions that can be promoted by these semiconductors. These positions, as given in Table 12.4, are for the static state of the semiconductor under a semiconductor/vacuum interface. These redox values may be altered during the adsorption and activation of the reagents. This has partly been taken care of in the concept of band bending when the interface is changed to the reaction medium [42]. There is a possibility that the energy level positions of the bands of the semiconductor may functionally change depending on the reaction conditions employed. This aspect has not yet been fully and explicitly dealt within the literature.

It was pointed out earlier that the adsorption of carbon dioxide should be such that the band angle should reduce from 180° to a nearly tetrahedral angle. There can be various modes of adsorption of carbon dioxide on the catalyst surface, depending on the nature of the surface morphology. Essentially, the possible structural modes of adsorption of carbon dioxide can be visualized as shown in Figure 12.6 [3].

The modes shown in Figure 12.6 are the ideal configurations of the adsorption mode of carbon dioxide. Depending on the nature of the surface site and the adsorption geometry of the substrate, the modes of adsorption of CO_2 can vary and one typical configuration was shown in Figure 12.2. As already stated, the reduction of CO_2 is limited kinetically since the lowest unoccupied molecular orbital (LUMO) level is an antibonding orbital and hence the reduction process has to be coupled with proton transfer. For this purpose the qualitative molecular orbital energy diagram for carbon dioxide is as shown in Figure 12.7. The reduction of carbon dioxide to hydrocarbons can be carried out on surfaces where proton and electron transfers are simultaneously possible. Thus the search for catalyst systems should be carried out on such surfaces where the transfer is facile for both these species.

Carbon dioxide is chemically inert, has a closed shell electronic configuration, and is linear in structure. The addition of a single electron causes the necessary bond angle reduction and bends the molecule structure due to the repulsion between the added electron and the electron pairs on the oxygen atoms. This repulsion contributes to the high energy of the LUMO level of the carbon dioxide molecule and thus accounts for the low electron affinity of the molecule. This situation makes it virtually certain that no semiconductor is capable of transferring the single electron to a free CO_2 molecule; the reduction potential is around –1.90 V as stated above. Though single electron reduction thus experiences a higher energy barrier, the situation is manageable with

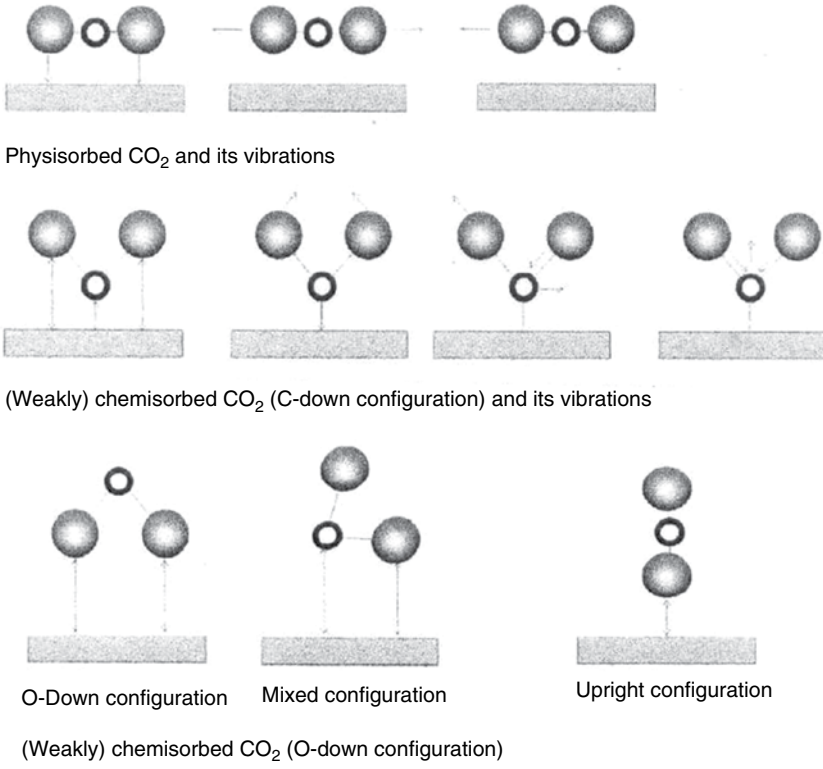

Figure 12.6 Possible adsorption modes (physisorbed, chemisorbed with C or O down) of carbon dioxide on surfaces. *Source:* Reproduced from Ref. [3].

proton-assisted transfer of multiple electrons. This is clear from the values of reduction potentials given in Table 12.2.

12.7 Perspectives in the Photocatalytic Reduction of Carbon Dioxide

In essence, the search for suitable semiconductor materials has been focusing on the following aspects:

1) Extending the photoresponse of the semiconductor to the visible region of the solar spectrum.
2) Sensitizing the semiconductor (by the addition of molecular species or coupling/modifying) to effectively utilize the excitons and improve the efficiency.

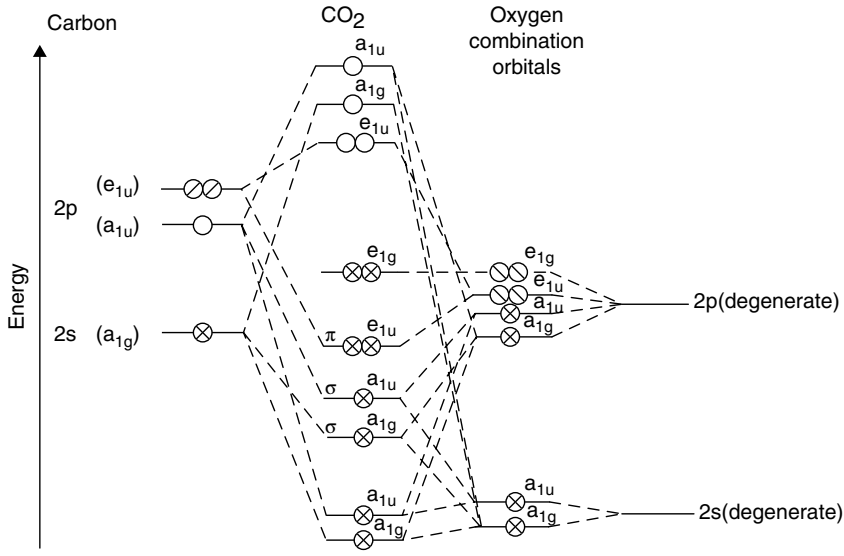

Figure 12.7 Qualitative molecular orbital diagram for carbon dioxide. *Source:* Reproduced from Ref. [3].

3) Altering the valence band maximum in order to change the value of the bandgap.
4) Altering the conduction band minimum to more reductive potential values so as to facilitate hydrogen production.
5) To generate multiple photocatalytically active sites and also to alter the surface area, new nanoscale morphologies have been employed.

In spite of these attempts, so far no realizable success in the reduction of carbon dioxide seems to have been achieved. This may mean that the steps so far attempted, though they may logically be in the correct direction, may only marginally improve the efficiency; perhaps the search has to take an alternative, so far untrodden, path.

At present, the formation rates of products from the photocatalytic reduction of carbon dioxide on semiconductors rarely exceed tens of $\mathrm{mmol\,g^{-1}\,h^{-1}}$. This means that the efficiency of the process is generally lower than in natural photosynthesis or even less than that achieved in the photocatalytic generation of hydrogen. However, this has not hampered the interest of scientists pursuing this research field.

Recent developments are concentrated on the search for new photocatalytic materials and new nanoscale configurations. New photocatalytic materials could be novel materials of metals with d^0 or d^{10} electronic configurations, though this concept that systems with this electronic configuration will be

appropriate semiconductors for this reaction has not yet been fully established. New nanoscale configurations could offer improved surface area, increased charge separation, and vectorial electron transfers. The mechanism of the process has been studied by both experimental and computational methods. These studies are aimed to answer the unanswered questions concerning the chemical pathways of CO_2 reduction. Of particular interest are the approaches to overcome the barrier associated with the activation of a CO_2 molecule toward the first one-electron reduction. This step is rate limiting, because of the highly negative electrochemical reduction potential of CO_2 to the anion radical with respect to the conduction band levels of commonly employed semiconductors. Other important aspects of the mechanism that are relevant for a deeper understanding of the process include charge-carrier dynamics within the semiconductors, the effect of the nanostructure of the photocatalyst, and the impact of the choice of the catalytic metal on the photocatalytic reduction of carbon dioxide. Most of the studies reported on this reaction employ TiO_2 and its variations [43, 44], as it is considered a good model system for comparative study.

The situation regarding the results reported about this system does not allow a direct comparison of the system as there is no standardized procedure adopted or assigned to report the results. It may be worthwhile if standardization could be achieved on the amount of the catalyst employed and also if there was a proper measure of the photon intensity employed. Another aspect on which there is no clarity or consistency is the counter reaction; this is the reaction involving oxygen or hydrogen peroxide formation in relation to the reduction reaction carried out. Until this is achieved, there will be always doubt on the sustainability of the reaction or long-term use of the catalysts for commercial exploitation. The system ultimately employed commercially should be based on the cost of the material and also that it is abundantly available.

Since ultimately the products of reaction should be separable, photoelectrochemical cells will be advantageous for exploiting this reaction commercially. The feverish attitude in studying this reaction and the consistent attempts to identify the appropriate semiconductors for promoting this reaction can be expected to move this process closer to success.

In the future, the direction of research may be to exploit the effects of mixed crystal phase, defect disorders, and modifications in designing the chosen catalyst systems. It is also necessary that the mechanistic details of the charge transfer will have to be elucidated with respect to details of each and every step at the interface.

Various configurations and various additives have been tried for the photocatalytic reduction of carbon dioxide. Varghese et al. [45] reported experiments conducted in outdoor sunlight. The relative hydrocarbon production rate of $111\,\mathrm{ppm\,cm^{-2}\ h^{-1}}$, or $\approx 160\,\mu\mathrm{l\,g^{-1}\ h^{-1}}$ has been reported when the nanotube array samples are loaded with both Cu and Pt nanoparticles. This rate of CO_2

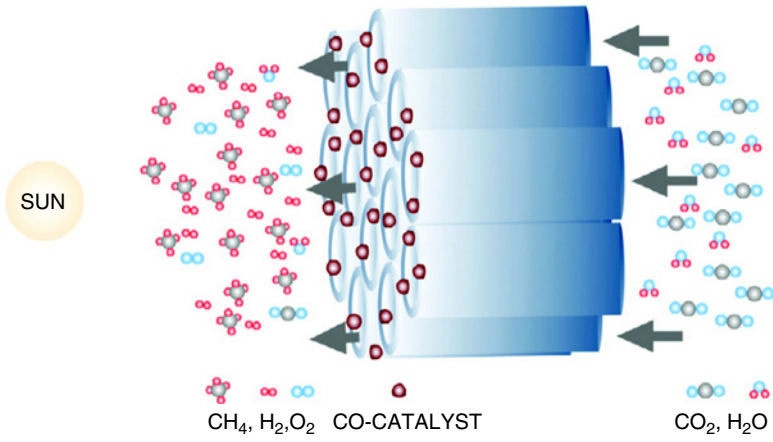

Figure 12.8 Flow through nanotube array loaded with co-catalyst for photocatalytic conversion of carbon dioxide and water into hydrocarbons. *Source:* Reproduced from Ref. [45].

to hydrocarbon production appears to be higher than what is so far reported. The pictorial representation of their system is shown in Figure 12.8.

Osterloh, in a recent commentary on recent advances in solar fuels and photocatalysis, said that this area continues to attract interest in the scientific community [46]. Solar photon energy can be used to form fuels. However, harnessing solar photons and utilizing their energy in technologically useful processes is not an easy job. It requires materials that are strong light absorbers, that exhibit long excited state lifetimes, and enable fast charge carrier processes.

As has been pointed out earlier, designing appropriate photocatalysts is important as it determines the activity and selectivity of CO_2 reduction. Nanostructuring resulted in increasing surface area and an increase in the number of active reaction sites, as pointed out earlier. In recent times interest has been focused on various configurations of composite photocatalysts by introducing metal and metal oxide co-catalysts, as well as Z-scheme systems [47]. These systems are mainly aimed to improve the charge separation. Additionally, Z-scheme photocatalytic systems have shown a strong tendency toward oxidation and reduction, while their narrow bandgap is beneficial to utilize visible light. Although various photocatalysts have shown good performance, the photocatalytic reduction of protons to hydrogen, a competitive reaction in aqueous CO_2 photoreduction, remains a major obstacle.

Significant improvements in catalyst and reactor design are needed for the photocatalytic functionalization of CO_2 to become a viable technology for the production of energy and chemicals. Fundamental strategies for the rational design of materials for effective transformations of CO_2 to value-added chemicals have to be evolved [48].

In recent times, a number of reviews and perspectives have been published in the literature on the photocatalytic reduction of carbon dioxide [49–51]. In spite of this spate of activity on this reaction, commercially viable processes are yet to evolve. The various reasons for this have been outlined.

The reasons for this failure can be many; however, the foremost among them is the choice of material. In the literature, various sensitization methods have been focused toward exploiting the visible range of the solar spectrum. However, even the utilization of the ultraviolet component of the solar spectrum (~3%) [52] alone may be enough to satisfy the energy needs of the Earth. Under these circumstances, the search for photocatalysts active in the visible spectrum has to be justified.

Secondly, the various sensitization methods employed in the fast five decades have not yielded the desired results. Hence, this may mean that the search for the selection of suitable materials must be directed elsewhere.

In conclusion, in spite of the various tools (both experimental and theoretical) on hand and also having the facility to scan a number of samples at the same time (high throughput analysis), the appropriate material for photocatalytic reduction of carbon dioxide or hydrogen generation from water has not been achieved in the last five decades, though vigorous attempts have been directed to do so. This may mean that nature still holds her secrets, as in photosynthesis. In our anxiety to mimic nature, we have not yet learnt the ways in which nature performs her functions to satisfy all the needs of the humanity in a satisfactory manner.

Acknowledgement

The author's grateful thanks are due to his colleagues and to the Department of Science and Technology, Government of India, for the creation of the National Center for Catalysis Research at the Indian Institute of Technology, Madras.

References

1 Aulice Scibioh, M. and Viswanathan, B. (2007). Carbon dioxide a matter of pollution or profit? *Consulting Ahead* 1 (2): 56–71.
2 (a)Aresta, M. (2003). *Carbon Dioxide Recovery and Utilization*. Springer;(b)Aresta, M. (2010). *Carbon Dioxide as Chemical Feedstock*. Wiley.
3 Aulice Scibioh, M. and Viswanathan, B. (2018). *Carbon Dioxide to Chemicals and Fuels*. Elsevier. ISBN: 9780444639967.
4 Wang, W.-N., Soulis, J., Jeffrey Yang, Y., and Biswas, P. (2014). Comparison of CO_2 photoreduction systems: a review. *Aerosol Air Qual. Res.* 14: 533–549.

5 Lehn, J.-M. and Ziessel, R. (1982). Photochemical generation of carbon monoxide and hydrogen by reduction of carbon dioxide and water under visible light irradiation. *Proc. Natl. Acad. Sci. U S A.* 79 (2): 701–704.

6 Zeng, S., Kar, P., Thakur, U.K., and Shankar, K. (2018). A review on photocatalytic CO_2 reduction using perovskite oxide nanomaterials. *Nanotechnology* 29: 1–22.

7 Inoue, T., Fujishima, A., Konishi, S., and Honda, K. (1979). Photoelectrocatalytic reduction of carbon dioxide in aqueous suspensions of semiconductor powders. *Nature* 277: 637–638. https://doi.org/10.1038/277637a0.

8 Halmann, M.M. and Steinberg, M. (1999). *Greenhouse Gas Carbon Dioxide Mitigation: Science and Technology*. Boca Raton: Lewis Publishers.

9 Hawecker, J., Lehn, J.-M., and Ziessel, R. (1983). Efficient photochemical reduction of CO_2 to CO by visible light irradiation of systems containing $Re(bipy)(CO)_3X$ or $Ru(bipy)_3^{2+}$–Co^{2+} combinations as homogeneous catalysts. *J. Chem. Soc. Chem. Commun.* 536–538. https://doi.org/10.1039/C39830000536.

10 Takeda, H., Koizumi, H., Okamoto, K., and Ishitani, O. (2014). Photocatalytic CO_2 reduction using a Mn complex as a catalyst. *Chem. Commun.* 50: 1491–1493. https://doi.org/10.1039/C3CC48122K.

11 Kuramochi, Y., Kamiya, M., and Ishida, H. (2014). Photocatalytic CO_2 reduction in *N*,*N*-dimethyl acetamide/water as an alternative solvent system. *Inorg. Chem.* 53: 3326–3332. https://doi.org/10.1021/ic500050q.

12 Tamaki, Y., Morimoto, T., Koike, K., and Ishitani, O. (2012). Photocatalytic CO_2 reduction with high turnover frequency and selectivity of formic acid formation using Ru(II) multinuclear complexes. *Proc. Natl. Acad. Sci. U. S. A.* 109: 15673–15678. https://doi.org/10.1073/pnas.1118336109.

13 Bruckmeier, C., Lehenmeier, M.W., Reithmeier, R. et al. (2012). Binuclear rhenium(I) complexes for the photocatalytic reduction of CO_2. *Dalton Trans.* 41: 5026–5037. https://doi.org/10.1039/c2dt30273j.

14 Lv, H., Song, J., Geletii, Y.V. et al. (2014). An exceptionally fast homogeneous carbon-free cobalt-based water oxidation catalyst. *J. Am. Chem. Soc.* 136: 9268–9271. https://doi.org/10.1021/ja5045488.

15 Tanaka, S., Annaka, M., and Sakai, K. (1653–1655). Visible light-induced water oxidation catalyzed by molybdenum-based polyoxometalates with mono-and dicobalt(III) cores as oxygen-evolving centers. *Chem. Commun.* 48: 2012. https://doi.org/10.1039/C2CC16821A.

16 Han, X.-B., Zhang, Z.-M., Zhang, T. et al. (2014). Polyoxometalate-based cobalt–phosphate molecular catalysts for visible light-driven water oxidation. *J. Am. Chem. Soc.* 136: 5359–5366. https://doi.org/10.1021/ja412886e.

17 Grills, D.C. and Fujita, E. (2010). New directions for the photocatalytic reduction of CO_2: Supramolecular, $ScCO_2$ or biphasic ionic liquid-$ScCO_2$ systems. *J. Phys. Chem. Lett.* 1: 2709–2718. https://doi.org/10.1021/jz1010237.

18 Hawecker, J., Lehn, J.M., and Ziessel, R. (1990–2012). Photochemical and electrochemical reduction of carbon dioxide to carbon monoxide mediated by (2,2′-bipyridine) tricarbonylchlororhenium(I) and related complexes as homogeneous catalysts. *Helv. Chim. Acta* 69: 1986. https://doi.org/10.1002/hlca.19860690824.

19 Haynes, W.M. (ed.) (2010). Solubility of carbon dioxide in water at various temperatures and pressures. In: *CRC Handbook of Chemistry and Physics*, 91e. Boca Raton: CRC Press. http://sites.chem.colostate.edu/diverdi/all_courses/CRC%20reference%20data/solubility%20of%20carbon%20dioxide%20in%20water.pdf (accessed 30 January 2019).

20 Lingampalli, S.R., Ayyub, M.M., and Rao, C.N.R. (2017). Recent progress in the photocatalytic reduction of carbon dioxide. *ACS Omega* 2: 2740–2748.

21 Habisreutinger, S.N., Schmidt-Mende, L., and Stolarczyk, J.K. (2013). Photocatalytic reduction of CO_2 on TiO_2 and other semiconductors. *Angew. Chem. Int. Ed.* 52: 7372–7408. https://doi.org/10.1002/anie.201207199.

22 Izumi, Y. (2013). Recent advances in the photocatalytic conversion of carbon dioxide to fuels with water and/or hydrogen using solar energy and beyond. *Coord. Chem. Rev.* 257: 171–186. https://doi.org/10.1016/j.ccr.2012.04.018.

23 (a) Wang, X., Li, Z., Shi, J., and Yu, Y. (2014). *Chem. Rev.* 114: 9346–9384.(b) Li, Y., Yang, X.Y., Feng, Y. et al. (2012). *Crit. Rev. Solid State Mater. Sci.* 37: 1–74.

24 (a) Zhang, X., Han, F., Shi, B. et al. (2012). *Angew. Chem. Int. Ed.* 51: 11778–11782.(b) Zhang, Z. and Antilla, J.C. (2012). *Angew. Chem.* 124: 11948–11952.

25 Feng, X., Sloppy, J.D., La Tempa, T.J. et al. (2011). *J. Mater. Chem.* 21: 13429–13433.

26 Rioux, R.M., Komor, R., Song, H. et al. (2008). *J. Catal.* 254: 1–11.

27 Sugano, Y., Shiraishi, Y., Tsukamoto, D. et al. (2013). *Angew. Chem. Int. Ed.* 52: 5295–5299; Angew. Chem. 125, 2013, 5403–5407.

28 Qing, K., Tao, W., Ping, L. et al. (2015). Photocatalytic reduction of carbon dioxide by hydrous hydrazine over Au–Cu alloy nanoparticles supported on $SrTiO_3/TiO_2$ coaxial nanotube arrays. *Angew. Chem. Int. Ed.* 54: 841–845.

29 Jiang, J., Li, H., and Zhang, L. (2012). New insight into daylight photocatalysis of AgBr@Ag: synergistic effect between semiconductor photocatalysis and plasmonic photocatalysis. *Chem. Eur. J.* 18: 6360–6369. https://doi.org/10.1002/chem.201102606.

30 Zhang, N., Liu, S., and Xu, Y.-J. (2012). Recent progress on metal core@semiconductor shell nanocomposites as a promising type of photocatalyst. *Nanoscale* 4: 2227–2238. https://doi.org/10.1039/c2nr00009a.

31 Chen, J.-J., Wu, J.C., Wu, P.C., and Tsai, D.P. (2010). Plasmonic photocatalyst for H_2 evolution in photocatalytic water splitting. *J. Phys. Chem. C* 115: 210–216. https://doi.org/10.1021/jp1074048.

32 An, C., Wang, R., Wang, S., and Zhang, X. (2011). Converting AgCl nanocubes to sunlight-driven plasmonic AgCl:Ag nanophotocatalyst with high activity

and durability. *J. Mater. Chem.* 21: 11532–11536. https://doi.org/10.1039/c1jm10244c.

33 Link, S. and El-Sayed, M.A. (1999). Spectral properties and relaxation dynamics of surface plasmon electronic oscillations in gold and silver nanodots and nanorods. *J. Phys. Chem. B* 103: 8410–8426. https://doi.org/10.1021/jp9917648.

34 Ghosh, S.K. and Pal, T. (2007). Interparticle coupling effect on the surface plasmon resonance of gold nanoparticles: from theory to applications. *Chem. Rev.* 107: 4797–4862. https://doi.org/10.1021/cr0680282.

35 Hong, J.D., Zhang, W., Ren, J., and Xu, R. (2013). Photocatalytic reduction of carbon dioxide – A brief review on product analysis and systematic methods. *Anal. Method* 5: 1086–1097.

36 Liang, L., Li, X., Sun, Y. et al. (2018). Infrared light-driven CO_2 overall splitting at room temperature. *Joule* 2: 1–13.

37 Kim, W., Seok, T., and Choi, W. (2012). Nafion layer-enhanced photosynthetic conversion of CO_2 into hydrocarbons on TiO_2 nanoparticles. *Energy Environ. Sci.* 5: 6066–6070.

38 Wallace, S.K., Mitzi, D.B., and Walsh, A. (2017). The steady rise of Kesterite solar cells. *ACS Energy Lett.* 2: 776–779.

39 Bhatkhande, D.S., Pangarkar, V.G., and Beenackers, A.A.C.M. (2001). Photocatalytic degradation for environmental applications – a review. *J. Chem. Technol. Biotechnol.* 77: 102–116, ISSN 0268-2575.

40 Indrakanti, V.P., Kubicki, J.D., and Schobert, H.H. (2009). Photoinduced activation of carbon dioxide on Ti-based heterogeneous catalysts, current state, chemical physics-based insights and out look. *Energy Environ. Sci.* 2: 745–758.

41 Jiang, Z., Xiao, T., Kuznetsov, V.I., and Edwards, P.P. (2010). Turning carbon dioxide into fuel. *Philos. Trans. R. Soc. A* 368: 3343–3364.

42 Zhang, Z. and Yates, J.T. Jr. (2012). Band bending in semiconductors: chemical and physical consequences at surfaces and interfaces. *Chem. Rev.* 112 (10): 5520–5551.

43 Chong, R., Caihong, S., Yuqing, D. et al. (2018). Insights into the role of MgAl layered double oxides interlayer in Pt/TiO_2 toward photocatalytic CO_2 reduction. *J. Catal.* 363: 92–101.

44 Liu, L. and Li, Y. (2014). Understanding the reaction mechanism of photocatalytic reduction of CO_2 with H_2O on TiO_2-based photocatalysts: a review. *Aerosol Air Qual. Res.* 14: 453–469.

45 Varghese, O.K., Paulose, M., La Tempa, T.J., and Crimes, C.A. (2009). High rate solar photovoltaic conversion of CO_2 and water vapour to hydrocarbon fuels. *Nano Lett.* 9: 731–737.

46 Osterloh, F.E. (2018). *Journal of Materials Chemistry A*: Editor's choice web collection: "Recent advances in solar fuels and photocatalysis research". *J. Mater. Chem. A* 6: 9763–9764.

47 Peng, C., Reid, G., Wang, H., and Hu, P. (2017). Perspective: photocatalytic reduction of CO_2 to solar fuels over semiconductors. *J. Chem. Phys.* 147: 030901.

48 Kondratenko, E.V., Mul, G., Baltrusaitis, J. et al. (2013). Status and perspectives of CO_2 conversion into fuels and chemicals by catalytic, photocatalytic and electrocatalytic processes. *Energy Environ. Sci.* 6: 3112–3135.

49 Sohn, Y., Huang, W., and Taghipour, F. (2017). Recent progress and perspectives in the photocatalytic CO_2 reduction of Ti-oxide-based nanomaterials. *Appl. Surf. Sci.* 396: 1656–1711.

50 Xie, S., Zhang, Q., Liu, G., and Wang, Y. (2016). Photocatalytic and photoelectrocatalytic reduction of CO_2 using heterogeneous catalysts with controlled nanostructures. *Chem. Commun.* 52: 35–59.

51 Ge, M., Cao, C., Huang, J. et al. (2016). A review of one-dimensional TiO_2 nanostructured materials for environmental and energy applications. *J. Mater. Chem. A* 4: 6772–6801.

52 Tsao, J., Lewis, N., and Crabtree, G. (2006). *Solar FAQs*. http://www.sandia.gov/~jytsao/Solar%20FAQs.pdf (accessed 30 January 2019).

53 Aulice Scibioh, M. and Viswanathan, B. (2004). Electrochemical reduction of carbon dioxide: a status report. *Proc. Indn. Natl. Acad. Sci.* 70A (3): 407–462.

54 Tan, S.S., Zou, L., and Hu, E. (2006). Photocatalytic reduction of carbon dioxide into gaseous hydrocarbon using TiO_2 pellets. *Catal. Today* 115: 269–273. https://doi.org/10.1016/j.cattod.2006.02.057.

55 Tan, S.S., Zou, L., and Hu, E. (2007). Photo-synthesis of hydrogen and methane as key components for clean energy system. *Sci. Technol. Adv. Mater.* 8: 89–92. https://doi.org/10.1016/j.stam.2006.11.004.

56 Akhter, P., Hussain, M., Russo, N., and Saracco, G., Photocatalytic reduction of CO_2 to methane, *XXXV Meeting of the Italian Section of the Combustion Institute*. http://www.combustion-institute.it/proceedings/XXXV-ASICI/papers/35proci2012.V2.pdf (accessed 30 January 2019).

57 Anpo, M., Yamashita, H., Ichinashi, Y., and Ehara, S. (1995). Photocatalytic reduction of CO_2 with H_2O on various titanium oxide catalysts. *J. Electroanal. Chem.* 396: 21–26. https://dx.doi.org/10.1016/0022-0728(95)04141-A.

58 Mori, K., Yamashita, H., and Anpo, M. (2012). Photocatalytic reduction of CO_2 with H_2O on various titanium oxide photocatalysts. *RSC Adv.* 2: 3165–3172.

59 Zhang, Q., Lin, C.-F., Jing, Y.H., and Chang, C.-T. (2014). Photocatalytic reduction of carbon dioxide to methanol and formic acid by graphene-TiO_2. *J. Air Waste Manage. Assoc.* 64: 578–585.

60 Liu, X., Ye, L., Liu, S. et al. Photocatalytic reduction of CO_2 by ZnO micro/nanomaterials with different morphologies and ratios of {0001} facets. *Sci. Rep.* 6: 38474. https://doi.org/10.1038/srep384.

61 Tong-ming, S., Qin, Z.-Z., Ji, H.-B. et al. (2015). Recent advances in the photocatalytic reduction of carbon dioxide. *Environ. Chem. Lett.* 14 (1): 99. https://doi.org/10.1007/s10311-015-0528-0.

62 Li, X., Liu, H., Luo, D. et al. (2012). Adsorption of CO_2 on heterostructure $CdS(Bi_2S_3)/TiO_2$ nanotube photocatalysts and their photocatalytic activities in the reduction of CO_2 to methanol under visible light irradiation. *Chem. Eng. J.* 180: 151–158.

63 Tahir, B., Tahir, M., and Amin, N.A.S. (2017). Photocatalytic carbon dioxide reduction to fuels over Cu-loaded g-C_3N_4 nanocatalyst under visible light. *Chem. Eng. Trans.* 56: 403–408.

64 Sayama, K. and Arakawa, H. (1993). Photocatalytic decomposition of water and photocatalytic reduction of carbon dioxide over ZrO_2 catalyst. *J. Phys. Chem.* 97: 531–533. https://doi.org/10.1021/j100105a001.

65 Al Otaibi, B., Fan, S., Wang, D. et al. (2015). Wafer-level artificial photosynthesis for CO_2 reduction into CH_4 and CO using GaN nanowires. *ACS Catal.* 5 (9): 5342–5348.

66 Kozah, O., Praus, P., Koci, K., and Klementora, M. (2010). Preparation and characterization of ZnS nanopartilces deposited on montmorillonite. *J. Colloid Interface Sci.* 352: 244.

67 Kumar, B., Llorente, M., Froehlich, J. et al. (2012). Photochemical and photoelectrochemical reduction of CO_2. *Annu. Rev. Phys. Chem.* 63: 541–569.

68 Wang, C., Thompson, R.L., Ohodnicki, P. et al. (2011). Size-dependent photocatalytic reduction of CO_2 with PbS quantum dot sensitized TiO_2 heterostructured photocatalysts. *J. Mater. Chem.* 21: 13452.

69 Aurian-Blajeni, B., Halmannjf, M., and Manasse, J. (1980). Photoreduction of carbon dioxide and water into formaldehyde and methanol on semiconductor materials. *Sol. Energy* 25: 165–170.

70 Stock, M. and Dunn, S. (2011). $LiNbO_3$ – a new material for artificial photosynthesis. *IEEE Trans. Ultrason. Ferroelectr. Freq. control* 58 (9): 1988–1993.

71 Li, M., Wang, J., Zhang, P. et al. Superior adsorption and photoinduced carrier transfer behaviors of dandelion-shaped Bi_2S_3@MoS_2: experiments and theory. *Sci. Rep.* 7: 42484. https://doi.org/10.1038/srep4248.

72 Handoko, A.D., Li, K., and Tang, J. (2013). Recent progress in artificial photosynthesis: CO_2 photoreduction to valuable chemicals in a heterogeneous system. *Curr. Opin. Chem. Eng.* 2: 200–206.

73 Viswanathan, B. and Aulice Scibioh, M. (2014). *Photoelectrochemistry: Principles and Practics*. Alpha Science International Limited.

74 Nahar, S., Zain, M.F.M., Kadhum, A.A.H. et al. (2017). Advances in photocatalytic reduction of CO_2 with water: a review. *Materials (Basel)* 10 (6): 629.

75 Viswanathan, B. (2012). Reflections on the electrochemical reduction of carbon dioxide on metallic surfaces. *Indian J. Chem. Sect. A* 51: 166–173.